cortex is the principle target of receptors in muscles (*11*). When area 3a recording sites were activated, they related to body locations that roughly corresponded to those activating adjoining recording sites in area 3b. Thus, our observations are consistent with the concept of a representation in area 3a that is parallel to that in area 3b, but further details are unclear.

We found that area 2 of the owl monkey was almost exclusively activated by stimulating deep body tissues. Because it was difficult to stimulate selectively restricted regions of deep receptors, it was possible to obtain only a crude idea of the organization of area 2 in this monkey. Yet it was clear that the overall organization of area 2 was in parallel with areas 3b and 1 and that body parts were represented for a third time in area 2. In macaque monkeys, area 2 responded to cutaneous as well as deep stimuli. We do not know if this difference between monkeys reflects a difference in the susceptibility of cutaneous input to suppression by anesthetics, but the difference did allow a more detailed analysis of the organization of area 2 in macaques. Progressions of receptive fields for rows of recording sites across areas 1 and 2 indicate a mirror reversal of somatotopic organization at the border (Fig. 2B). Thus, areas 3b and 1 and areas 1 and 2 are approximately mirror reversals of each other. The data from the many rows of recording sites that were typically obtained in each experiment made it also apparent that none of the three representations was a simple distortion of the body without splits or disruptions. Disruptions may be necessary for the distorted map to fit in an architectonic strip. However, it is important to note that the discontinuities are not predicted strictly by the dermatomal sequence, and that they differ in location in the separate representations.

We conclude that the classical primary somatosensory cortex consists of four functionally distinct strips. At least areas 3b, 1, and 2 contain separate body representations. We believe this interpretation is required by the mapping data. Furthermore, the multiple representations hypothesis is clearly more consistent with the microelectrode studies that indicate that each architectonic area has its own pattern of sensory activation (*5, 7, 8, 11*), recent anatomical studies that demonstrate distinctive patterns of connections for each of the architectonic fields (*8, 12*), and ablation-behavioral investigations showing specific impairment associated with lesions restricted to specific fields (*13*). There is little doubt that the four fields 3a, 3b, 1, and 2—and not SI—are the subdivisions of functional significance of the parietal somatosensory cortex of monkeys, and perhaps of all higher primates.

JON H. KAAS
Department of Psychology, Vanderbilt University, Nashville, Tennessee 37240
RANDALL J. NELSON
Department of Anatomy, Vanderbilt University
MRIGANKA SUR
Department of Electrical Engineering, Vanderbilt University
CHIA-SHENG LIN*
Department of Anatomy, Vanderbilt University
MICHAEL M. MERZENICH
Coleman Laboratory, University of California, San Francisco 94143

References and Notes

1. W. H. Marshall, C. N. Woolsey, P. Bard, *Science* **85**, 388 (1937); C. N. Woolsey, W. H. Marshall, P. Bard, *Bull. Johns Hopkins Hosp.* **70**, 399 (1942).
2. C. N. Woolsey and D. Fairman, *Surgery* **19**, 684 (1946).
3. K. Brodmann, *Vergleichende Lokalizationslehre der Grosshirnride* (Barth, Leipzig, 1909). The subdivision of Brodmann's area 3 into 3a and 3b was first made on myeloarchitectonic bases by O. Vogt [*J. Psychol. Neurol. (Leipzig)* **25**, 279 (1919)].
4. C. N. Woolsey, in *The Biology of Mental Health and Disease* (Hoeber, New York, 1952), pp. 193–203; in *Biological and Biochemical Bases of Behavior*, H. F. Harlow and C. N. Woolsey, Eds. (Univ. of Wisconsin Press, Madison, 1958), pp. 63–81; in *Cerebral Localization and Organization*, G. Schaltenbrand and C. N. Woolsey, Eds. (Univ. of Wisconsin Press, Madison, 1964), pp. 17–26; ——, R. Tasker, C. Welt, R. Ladpli, G. Campos, H. P. Potter, R. Emmers, H. Schwassman, *Trans. Am. Neurol. Assoc.* **85**, 144 (1960).
5. T. P. S. Powell and V. B. Mountcastle, *Bull. Johns Hopkins Hosp.* **105**, 133 (1959); V. B. Mountcastle and T. P. S. Powell, *ibid.*, p. 173.
6. B. H. Pubols and L. M. Pubols, *Brain Behav. Evol.* **5**, 342 (1972); G. Werner and B. L. Whitsel, *J. Neurophysiol.* **31**, 856 (1968); B. L. Whitsel, D. A. Dreyer, J. R. Ropolo, *ibid.* **34**, 1018 (1971); D. A. Dreyer, R. J. Schneider, C. B. Metz, B. L. Whitsel, *ibid.* **37**, 119 (1974); D. A. Dreyer, P. R. Loe, C. B. Metz, B. L. Whitsel, *ibid.* **38**, 714 (1975).
7. R. L. Paul, M. Merzenich, H. Goodman, *Brain Res.* **36**, 229 (1972); R. L. Paul, H. Goodman, M. Merzenich, *ibid.* **39**, 1 (1972).
8. M. M. Merzenich, J. H. Kaas, M. Sur, C.-S. Lin, *J. Comp. Neurol.* **181**, 41 (1978).
9. Our studies also include 1800 recording sites in ten prosimian primates (*Galago senegalensis* and *Galago crassicaudatus*). Only one low-threshold cutaneous representation was found, although cortex rostral and caudal to this representation was responsive to more intense stimuli. These observations are consistent with those of two other recent microelectrode mapping studies in prosimians [A. Krishnamurti, F. Sanides, W. I. Welker, *Brain Behav. Evol.* **13**, 367 (1976); M. Carlson and C. Welt, *Soc. Neurosci. Abstr.* **3**, 478 (1977)]. The organization of the low-threshold representation identifies it as the 3b field. We are still uncertain whether areas 1 and 2 exist in prosimians.
10. We did not find that the digits in area 1 of macaque monkeys face rostrally, in the same direction as in area 3b as reported by Paul *et al.* (*7*). It is possible that Paul *et al.* attributed data from area 2, where the digits do point rostrally, to area 1 where the digits point caudally (Fig. 2).
11. C. G. Phillips, T. P. S. Powell, M. Wiesendanger, *J. Physiol. (London)* **217**, 419 (1971); G. E. Lucier, D. C. Ruegg, M. Wiesendanger, *ibid.* **251**, 388 (1975); J. Tanji, *Brain Res.* **88**, 549 (1975); G. J. Heath, J. Hore, C. G. Phillips, *J. Physiol. (London)* **257**, 199 (1976); P. Zarzechi, Y. Shinada, H. Asanuma, *Soc. Neurosci. Abstr.* **2**, 1388 (1976).
12. B. A. Vogt and D. N. Pandya, *J. Comp. Neurol.* **177**, 179 (1978); E. G. Jones, *ibid.* **160**, 167 (1975); J. D. Coulter and S. H. C. Hendry, *ibid.* **181**, 291 (1978).
13. M. Randolph and J. Semmes, *Brain Res.* **70**, 55 (1974).
14. J. M. Allman and J. H. Kaas, *Science* **191**, 572 (1976); T. J. Imig, M. A. Ruggero, L. M. Kitzes, E. Javel, F. F. Brugge, *J. Comp. Neurol.* **171**, 111 (1977).
15. This research was supported by grant BNS 76-81824 from the National Science Foundation and grant NS-10414 from the National Institutes of Health.
* Present address: Department of Physiology, University of Virginia Medical School, Charlottesville 22901.

25 October 1978; revised 26 December 1978

Intraretinal Distribution of Cone Pigments in Certain Teleost Fishes

Abstract. *Microspectrophotometric investigations of visual pigments in the teleost family Cichlidae determined that morphological "twin cones" need not be "pigment twins" as well. In each species there were two pigments that could be found in these cells; a "longwave" and a "shortwave" type whose precise spectral location varies for each species, making the terms red and green inadequate to describe them. Studies of the receptor mosaic with the nitro-blue tetrazolium chloride reduction technique permitted the sampling of larger receptor populations and confirmed that twin cones in several cichlid species could be either longwave-longwave, longwave-shortwave, or shortwave-shortwave pairs, and that the relative proportions of these twin cone types vary in different parts of the retinas. Nonuniform distribution of pigment types was also evident in the eyes of several other species from a variety of piscine taxa.*

The retinas of many fish species exhibit single, double, and twin cones. Double cones, such as those described in the goldfish (*Carassius auratus*), are characterized by members of dissimilar appearance in both fixed and fresh preparations. One member of the pair has an ellipsoid body and an outer segment which are broader and longer than those of the other member. This cell usually contains

0036-8075/79/0504-0523$00.50/0 Copyright © 1979 AAAS

a more longwave-sensitive pigment than the shorter cell (*1*). This observation has been extended to include at least nine other families of fishes (*2*).

In the goldfish, such double cones are called red-green pairs. Since the spectral locations of the pigments vary widely in the numerous teleosts we have studied, we find that the terms red and green are inadequate and misleading. The terms longwave and shortwave paired cone pigments (PCP's) are used in this report.

The single cones that are present in many species usually (but not always) contain a third pigment with a sensitivity maximum (λ_{max}) at still shorter wavelengths.

In most teleosts, the visual cells are arranged in one of a number of regular mosaic patterns (*3*). In goldfish, the pigment array displays the chromatic organization predicted from the physical arrangement of the cells (*4*).

Complications arise, however, when discussing the retinas of cichlids, percids, centrarchids, and several other groups. Paired cones in these species may not be obvious morphological doubles or twins in either fresh or fixed preparations for light microscopy. Cell pairs that appear to be morphological doubles may be pigment twins, and putative morphological twins may contain different pigments. Studies with the rapid scan photon-counting microspectrophotometer (PMSP) (*5*) showed that, while unquestionable double cones usually exhibited the same pattern as those of the goldfish, apparent twins could consist of a longwave member and a shortwave member (LS pairs), two longwave cells (LL pairs), or two shortwave cells (SS pairs). Attempts by the PMSP operator to predict the pigment content of these dubious twins strictly from their appearance in fresh preparations met with random success.

Early in these investigations it was noted that when small (about 1 mm²) samples were taken from large (about 1 cm in diameter) eyes, the proportions of LL, LS, and SS pairs varied extensively from sample to sample. Pieces from the dorsal retina near the periphery consisted mainly of LL pairs (LL:LS ratio approximately 3:1). Certain other retinal areas were composed predominantly of LS pairs, while samples from parts of the ventral retina contained all three types at the same time (LL:LS:SS ratio, approximately 1:2:2). Sampling of cell populations by PMSP in this manner is both time-consuming and subject to bias, however, so that little more than the above could be determined.

To clarify the situation we used the nitro-blue tetrazolium chloride reduction technique (*6*) on two species of cichlids, *Cichlasoma longimanus* and *Heterotilapia multispinosa*. This vital staining technique causes the deposition of dark blue nitro-blue tetrazolium diformazan (NBT-DF) in the mitochondria-filled el-

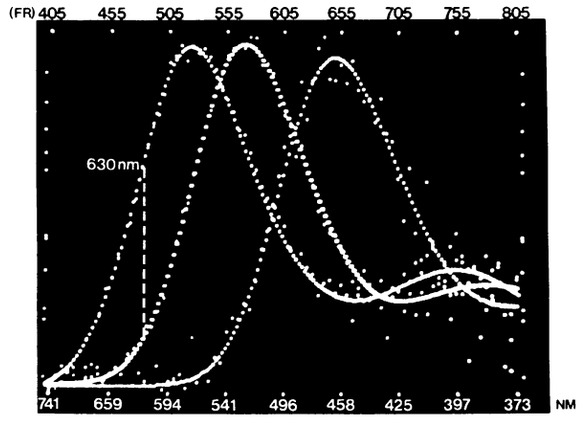

Fig. 1. Visual pigments of the cichlid fish *Cichlasoma longimanus* as determined by transverse measurements with the PMSP, plotted on a linear frequency axis. These curves represent the averages of a number of records for each cell type, fitted with template curves. Absorption maxima for this species are 579 ± 5 nm and 531 ± 2 nm (found in paired cones), and 455 ± 5 nm (found in single cones only). Curves are normalized and indicate relative density as a function of frequency. Actual (transverse) optical densities ranged from 0.04 to 0.06. Dots at upper and lower margins indicate spectral location at 50-fresnel intervals. Upper row is labeled in frequency units (fresnels), lower row in wavelength units (nanometers). With these data, light of modal wavelength 630 nm was chosen for retinal irradiation in order to maximize the difference in degree of activation between the 579 and 531 pigments, while leaving the 455 pigment and the rods unaffected.

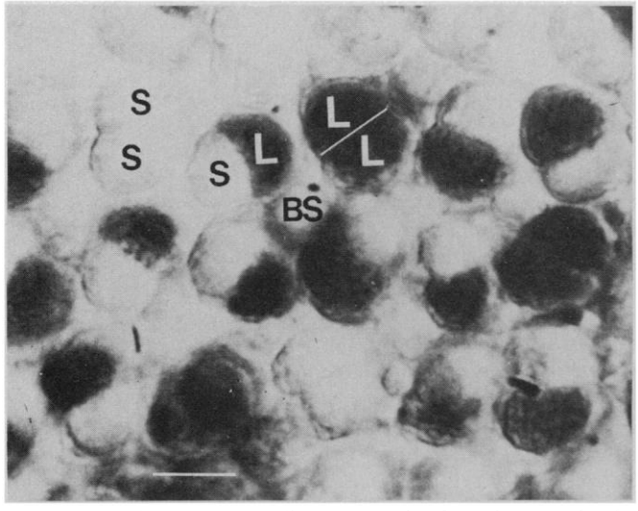

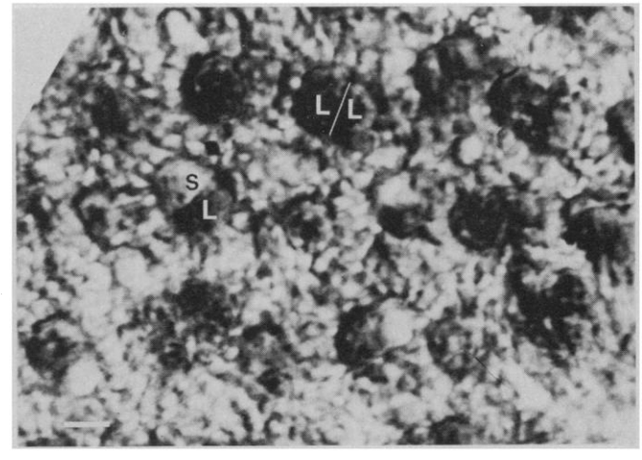

Fig. 2 (left). Nitro-blue tetrazolium preparation from the ventral retina of *Cichlasoma longimanus*, irradiated at 630 nm. Cells which appear dark have accumulated a mixture of NBT-HF and NBT-DF in the mitochondria-filled ellipsoid region as a result of altered metabolic activity. These are assumed to be cells containing the 579-nm (longwave double cone) pigment. Double cone pairs may both be dark (LL), both unstained (SS), or LS. Single Cones (*BS*), which always contain the blue (455 nm) pigment, never show any accumulation of stain (scale, 10 μm). Fig. 3 (right). Nitro-blue tetrazolium preparation from the dorsal retina of *Heterotilapia multispinosa*. The visual pigments in this species have λ_{max} values of 588 and 545 nm (double cones), and 466 nm (single cones). The irradiation wavelength was 630 nm. Note the absence of SS pairs, the higher relative proportion of LL pairs, and the absence of staining in single cones. Smaller objects between cone cells are rod outer segments (scale, 10 μm).

lipsoids of cells that have been metabolically altered by the bleaching of visual pigment in their outer segments. Once the absorbance spectra of the visual pigments in a species are known, it is possible selectively to activate (and hence stain) specific pigment classes of cells by selecting wavelength for irradiation of the retina (*7*).

The visual pigments in each species were first characterized with the PMSP. Data for each pigment type were averaged and fitted by eye to a template formed by generating the sum of three Gaussian functions (*8*) through the use of an interactive computor program. (This can only be done when the data are plotted on a linear frequency scale.) With these data as guides, a wavelength for retinal stimulation was chosen for each species to maximize the difference in degree of activation between cells containing the longwave and shortwave PCP's (Fig. 1). Stimuli were provided by a modified Leiss quartz prism monochromator (*9, 10*). Exposure times were controlled with a photographic enlarger timer to deliver roughly the total photon flux values determined to be most effective (*7*).

Our early efforts to use the NBT technique (*7*) indicated that changes in the method were necessary to facilitate its use on our chosen species. Experimental animals were maintained in the dark for at least 36 hours prior to the experiment. After enucleation, the corneas and lenses were removed, and the posterior eyecups were hemisected just dorsal to the optic disk. These dissections were performed in a low-calcium Ringer solution (*11*) to facilitate subsequent detachment of the sensory retina from the pigment epithelium. Irradiation of these basically intact preparations was followed by immediate removal of the sensory retina to the NBT-containing incubation medium (*12*) for 5 to 10 minutes at 32°C. Preparations were subsequently stabilized in the dark for 10 minutes in 10 percent formalin. Small pieces of retina were then mounted, receptor-side up, on slides sealed with silicone oil for observation under the Nomarski interference microscope. Photographs were taken with a Polaroid camera attachment. As was reported earlier (*7*), the preparation could be stored for several weeks without noticeable deterioration.

The thickness of these particular preparations necessitated extensive focusing in the plane perpendicular to the photoreceptors in order to completely visualize the receptor mosaic. Clear photographs were difficult to obtain because of the limited depth of field, despite the fact

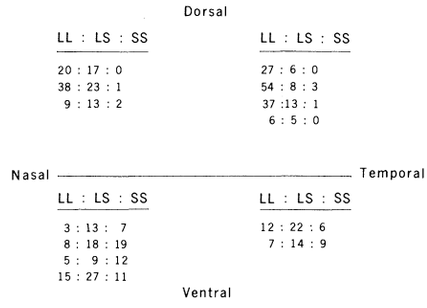

Fig. 4. Distribution of the three classes of paired cones in the retina of *Cichlasoma longimanus* by quadrant. L.L., longwave-longwave pair; LS, longwave-shortwave pair; SS, shortwave-shortwave pair.

that the patterns of staining were quite clear-cut to the observers. An area from the ventral retina of *Cichlasoma longimanus* (Fig. 2) was exposed to a total photon flux of 4×10^6 photon/μm^2 at a modal wavelength of 630 nm. Several typical morphological units are visible, each composed of four pairs of "twin" cones surrounding a central single cone. Those cells with heavy accumulations of NBT-DF are assumed to contain the longwave PCP. Neither the shortwave PCP-bearing cells nor the single cones (which were previously determined to contain a blue-sensitive pigment with λ_{max} at 455 nm) show any accumulation of stain.

The paired cones show no regular chromatic organization to match their physical mosaic arrangement. In any particular mosaic unit, virtually any combination of LL, LS, and SS pairs could be found. A few exhibited the regular alternating pattern described for the goldfish. A substantial number of cells in the ventral retina of this species are of the SS type (Fig. 2). In contrast, the dorsal retinas of both species were composed predominantly of LL pairs (Fig. 3), in agreement with the initial MSP results.

Sufficient samples were obtained from the retinas of *H. multispinosa* to permit the estimation of relative receptor populations in four quadrants of the retina, divided as shown in Fig. 4. Within each quadrant counts of each class of paired cones were taken in as many areas as possible. Difficulties in handling the material in general, and in obtaining clear views of the mosaic pattern in particular, made more accurate localization of the areas counted impossible. Since the clearly visible areas varied in size, the total number of cells counted in each sample also varied, but the general pattern is clear. Longwave PCP-containing cells are more numerous in the dorsal quadrants, while shortwave PCP-containing cells are more numerous in the ventral part of the eye.

This phenomenon of differential pigment distribution is not restricted to the Cichlidae. Such differences are widespread among aquatic vertebrates, including species as widely separated phylogenetically as the osteoglossomorph *Notopterus* (knife fish) and the poeciliid *Poecilia reticulata* (guppy). Although we have not yet been successful in obtaining clear-cut NBT preparations from these species, the MSP data provide strong evidence. The notopterids, which exhibit visual pigments similar to those of the cichlid PCP's in spectral position (*13*), have unusual retinas in which large numbers of rods and cones are grouped into common bundles (*14*). No differentiation into double, twin, or single cones was visible within these bundles, but spectra could be taken with little difficulty. In the bundles of the dorsal retina, the longwave pigment of the species predominates, while the shortwave pigment is found in the majority of cells in the ventral retina.

Guppies (and other poeciliids studied) have a set of visual pigments with λ_{max} values at unusually short wavelengths for freshwater species, which usually have a dehydroretinal chromophore and hence absorb at longer wavelengths. The guppy pigments have λ_{max} values of 546, 468, and 408 nm. Morphological studies (*15*) and our MSP work indicate that there is an area in the ventral retina of these fish where the paired cones are indeed twins. These cells and the "long single cones" that are present along with them in this region all contain the longwave PCP for the species.

The adaptive significance of these arrangements is far from clear, but merits comparison with what little is known about the underwater photic environment. Data on the transmission properties of various types of freshwater are sparse (*16*). However, in both riverine and lacustrine environments the transmission maximum is shifted toward the longwave end of the spectrum, away from the 480-nm maximum of pure fresh or salt water. Additionally, the farther light travels through an aquatic color filter, the more closely its $\lambda p50$ (*17*) approaches the transmission maximum of the medium (*18*). In turbid shallow-water environments, which transmit longwave light most readily, the upwelling and horizontally scattered spacelight will thus be redder than the downwelling illumination.

The shortwave PCP's of the cichlid species, with λ_{max} of 531 and 545 nm, are probably well situated spectrally to

match the λp50 of the downwelling illumination in the rivers and lakes of South America where they are found. A visual pigment matched in this way would maximize the apparent contrast when viewing objects silhouetted against the downwelling light. There are proportionally more cells containing the shortwave PCP's in the upward-looking ventral retina. The longwave PCP's are more common in the down and forward-looking dorsal retinas whose field of view contains a higher proportion of longwave light. The λ_{max} of the guppy longwave pigment is only 546 nm, rather close to the "shortwave" PCP of the cichlids and notopterids, is concentrated in the same area of the retina, and could function in a similar manner. The functional significance of the ellipsosomes contained in certain of the cones of poeciliids has yet to be determined (*19*).

If such intraretinal specializations occur in most fishes, they might provide a partial explanation for certain discrepancies encountered in studies of piscine color vision. Radically different photopic spectral sensitivities are often obtained for the same species when behavioral methods that differ in the location of the stimulus in the visual field are compared.

The differential distribution of colored oil droplets in the retinas of pigeons (*20*), while operating on a different principle, results in similar alterations of the relative spectral sensitivities of dorsal and ventral regions.

J. S. LEVINE
Museum of Comparative Zoology, Harvard University, Cambridge, Massachusetts 02138, and *Laboratory of Sensory Physiology, Marine Biological Laboratory, Woods Hole, Massachusetts 02543*
E. F. MACNICHOL, JR.
Laboratory of Sensory Physiology, Marine Biological Laboratory, Woods Hole and *Department of Physiology, Boston University School of Medicine Boston, Massachusetts 02118*
T. KRAFT
Massachusetts Institute of Technology, Cambridge
B. A. COLLINS
Laboratory of Sensory Physiology, Marine Biological Laboratory, Woods Hole

References and Notes

1. W. B. Marks, *J. Physiol. (London)* **178**, 14 (1965); M. A. Ali, F. I. Hárosi, H.-J. Wagner, *Sensory Proc.*, in press.
2. Polypteridae, Lepisosteidae, Amiidae, Gasteropelicidae, Hemiodontidae, Poecilidae, Cyprinodontidae, Belontiidae, Characidae; J. S. Levine, in preparation.
3. H.-J. Wagner, *Z. Morphol. Tiere* **72**, 77 (1972).
4. R. E. Marc and H. G. Sperling, *Science* **191**, 487 (1976).
5. E. F. MacNichol, Jr., *Invest. Ophthalmol.* (Suppl.), (April 1977), p. 118 (abstr.); in *Frontiers in Visual Science*, S. J. Cool and E. L. Smith, Eds. (Springer-Verlag, New York, 1978), pp. 194–208.
6. J. M. Enoch, *J. Opt. Soc. Am.* **54**, 368 (1964).
7. R. E. Marc and H. G. Sperling, *Vision Res.* **11**, 1211 (1976).
8. F. I. Harosi, *J. Gen. Physiol.* **68**, 65 (1976).
9. Courtesy of Dr. Albert Szent-Györgyi.
10. The prism of a Leiss quartz prism monochromator was replaced with a 600 groove/mm reflection grating blazed for 400 nm. The much greater dispersion of the grating allows the use of wide entrance and exit slits to illuminate an area of approximately 1 cm^2 with a flux of greater than 200 $\mu W/cm^2$, while retaining a narrow passband.
11. Our low-calcium Ringer solution contained 113.5 m*M* NaCl, 11.9 m*M* $NaHCO_3$, 3.3 m*M* NaH_2PO_4, 3.4 m*M* KCl, 21 m*M* $MgCl_2$, 11.1 m*M* glucose, adjusted to *p*H 7.4.
12. The composition of NBT incubation medium (*7*) was 39.0 m*M* NaCl, 0.7 m*M* KCl, 0.7 m*M* $CaCl_2$, 0.4 m*M* $MgSO_4$, 0.4 m*M* $NaHCO_3$, 5.5 m*M* NaH_2PO_4, 21.0 m*M* Na_2HPO_4, 6.0 m*M* NBT, and 13.0 m*M* disodium succinate.
13. The λ_{max} was 594 and 548 nm (J. S. Levine, in preparation).
14. M. A. Ali and M. Anctil, *Retinas of Fishes: An Atlas* (Springer-Verlag, New York, 1976).
15. Y. W. Kunz and C. Wise, *Experientia* **34**, 246 (1978); Y. W. Kunz, personal communication.
16. J. A. S. Kinney, S. M. Luria, D. O. Weitzman, *J. Opt. Soc. Am.* **57**, 802 (1967).
17. W. N. McFarland and F. W. Munz, *Vision Res.* **15**, 1063 (1975). While realizing the difficulty in attempting to characterize underwater spectra by a single number, McFarland and Munz realized the necessity for such an index to facilitate discussion. They proposed the term "λp50" to denote the wavelength which halves the total number of photons between 400 and 750 nm to describe the energy distribution of underwater spectra in a way which accurately relates to their effect on visual pigments.
18. ———, *ibid.*, p. 1071; F. W. Munz and W. N. McFarland, *Handbook of Sensory Physiology*, (Springer-Verlag, New York, 1978), vol. 7, part 5, pp. 193–274.
19. E. F. MacNichol, Jr., Y. W. Kunz, J. S. Levine, F. I. Hárosi, B. A. Collins, *Science* **200**, 549 (1978).
20. J. K. Bowmaker, *Vision Res.* **17**, 1129 (1977).
21. We thank the Rowland Foundation and other nongovernmental donors for generous support. D. M-K. Lam was instrumental in the development of the low-calcium bath technique. We thank A. Fein for advice and criticism. Cichlids were obtained through the courtesy of K. McKaye.

12 July 1978; revised 25 October 1978

Human Skin Fibroblasts Derived from Papillary and Reticular Dermis: Differences in Growth Potential in vitro

Abstract. *Papillary fibroblasts, when compared to reticular fibroblasts from the same skin specimen, exhibit greater proliferative capacities in vitro. These results demonstrate a difference in function between morphologically similar cells obtained from the same tissue. Such findings represent an important consideration in the study of cell aging in vitro.*

Fibroblastlike cell lines derived from human dermis are being extensively used in the diagnosis of genetic disorders as well as studies in vitro of the aging process (*1*). Investigators have presumed that those cell lines derived from the dermis of normal individuals will behave similarly when propagated in vitro. However, recent data have raised the possibility that normal human dermis contains several fibroblastlike cells which may differ in behavior while retaining similar morphology. For example, different responses to hydrocortisone were observed among fibroblastlike cell lines from a common site in normal individuals (*2*); qualitative differences in testosterone metabolism exist between sister lines derived from a single foreskin explant (*3*); and finally, both precursor forms of collagens I and III are synthesized by human skin fibroblasts cultured from the same biopsy (*4*).

In obtaining specimens for the study of

Table 1. Population doublings of human skin fibroblasts at passage four.

Normal fibroblast cell line	Age	Race	Sex	Site	PD*		Δ†
					Papillary	Reticular	
9	48	W	M	Thigh	7.8	5.3	−32.1
14	50	W	M	Thigh	8.3	7.2	−13.3
16	48	W	M	Abdomen	7.6	6.8	−10.5
17	63	W	M	Abdomen	7.4	4.0	−45.9
19	49	B	F	Buttock	8.1	6.2	−23.5
23	16	W	F	Abdomen	10.0	9.1	− 9.0
32	68	B	F	Abdomen	8.7	7.8	−10.3
33	19	W	F	Thigh	12.2	10.5	−13.9
40	79	B	F	Abdomen	9.8	8.8	−10.2
44	67	B	M	Abdomen	11.3	10.5	− 7.1
48	66	B	M	Abdomen	9.8	8.4	−14.0
50	32	W	M	Thigh	10.7	8.9	−17.0
52	45	W	F	Thigh	11.1	8.9	−20.0
Mean							−17.4

*The PD's were calculated by the equation $\log_2 \times (N/N_0)$ where N is the final cumulative cell number and N_0 is the initial cell number. †Δ = (PD reticular − PD papillary/PD papillary) × 100 percent.

0036-8075/79/0504-0526$00.50/0 Copyright © 1979 AAAS